Prefrontal inputs to the amygdala instruct fear extinction memory formation

Olena Bukalo[1,2,*], **Courtney R. Pinard**[1], **Shana Silverstein**[1,2], **Christina Brehm**[3], **Nolan D. Hartley**[4], **Nigel Whittle**[3], **Giovanni Colacicco**[1], **Erica Busch**[1], **Sachin Patel**[4], **Nicolas Singewald**[3], and **Andrew Holmes**[1]

[1]Laboratory of Behavioral and Genomic Neuroscience, National Institute on Alcohol Abuse and Alcoholism, National Institutes of Health, Bethesda, MD 20853, USA.

[2]Center for Neuroscience and Regenerative Medicine at the Uniformed Services University of the Health Sciences, Bethesda, MD 20814, USA.

[3]Department of Pharmacology and Toxicology, Institute of Pharmacy and Center for Molecular Biosciences Innsbruck, University of Innsbruck, Innrain 80-82/III, A-6020 Innsbruck, Austria.

[4]Department of Psychiatry and Molecular Physiology and Biophysics, Vanderbilt University Medical Center, Nashville, TN 37232, USA.

Abstract

Persistent anxiety after a psychological trauma is a hallmark of many anxiety disorders. However, the neural circuits mediating the extinction of traumatic fear memories remain incompletely understood. We show that selective, in vivo stimulation of the ventromedial prefrontal cortex (vmPFC)–amygdala pathway facilitated extinction memory formation, but not retrieval. Conversely, silencing the vmPFC-amygdala pathway impaired extinction formation and reduced extinction-induced amygdala activity. Our data demonstrate a critical instructional role for the vmPFC-amygdala circuit in the formation of extinction memories. These findings advance our understanding of the neural basis of persistent fear, with implications for posttraumatic stress disorder and other anxiety disorders.

INTRODUCTION

Anxiety disorders, trauma and stress-related disorders, and phobias (1) are highly prevalent psychiatric conditions that are still inadequately treated. Recent years have seen rapid

*Corresponding author. bukalool@mail.nih.gov.

advances in the understanding of the neural basis of pathological anxiety and the learning processes that underlie anxiety responses associated with a traumatic event, such as fear conditioning and extinction (2–6). However, there remain outstanding questions regarding the critical functional brain circuits that regulate the formation and extinction of fear memories.

Previous studies have shown that successful fear extinction in rodents is associated with robust activity in the ventromedial prefrontal cortex (vmPFC) (notably, the infralimbic cortex), the medial intercalated cell nuclei of the amygdala (mICNs), and a subpopulation of basolateral amygdala (BL) "extinction" neurons, whereas deficient extinction corresponds to sustained activity in the prelimbic cortex (PL) and a subset of BL ("fear") neurons (2, 4–8). Furthermore, electrically or pharmacologically stimulating the vmPFC is found to strengthen extinction in parallel with changes in the excitability and plasticity of BL and mICN neurons, whereas vmPFC lesions or inactivation disrupts extinction and attenuates BL-to-ICN-driven inhibition of central medial amygdala (CeM) output (9–15).

Collectively, these prior findings propose a model whereby inputs from the vmPFC to the amygdala support the formation of extinction memories and/or gate the expression of these memories. However, previous experimental manipulations either lack precise temporal control over the circuit or affect vmPFC projections not only to the amygdala but also to other target regions implicated in fear, such as the hippocampus, striatum, and midbrain (16, 17). Therefore, to provide a causal test of the contribution of the vmPFC-amygdala circuit to extinction, we used in vivo optogenetics to selectively stimulate or silence vmPFC inputs to the amygdala as mice acquired or retrieved an extinction memory.

RESULTS AND DISCUSSION

To control the vmPFC-amygdala circuit, we infected glutamatergic vmPFC projection neurons with adenoassociated virus (AAV) carrying either the light-sensitive cation-conducting opsin, channelrhodopsin-2 (ChR2) [rAAV5–calcium/calmodulin-dependent protein kinase IIa (CamKIIa)–hChR2(H134R)–enhanced yellow fluorescent protein (eYFP)], or the light-driven outward proton pump, archaerhodopsin-3 (ArchT) (rAAV5-CamKIIa-eArchT3.0-eYFP) (Fig. 1, A and C). Given the role of the PL in generating fear and opposing extinction (18), we removed those mice in which posttest histological analysis indicated that there was more than marginal virus spread into this region, although it remains likely that at least some portion of PL neurons were infected in the current study. Confirming the successful incorporation of functional opsins into vmPFC neurons, in vivo recordings from chronically implanted multielectrode arrays confirmed that shiningbluelight onChR2-expressing vmPFC cells increased local neuronal firing [t test: $t(52) = 3.32$, $P < 0.01$ versus pre-light, $n = 54$ units] (Fig. 1B), whereas shining green light inhibited local neuronal firing of ArchT-infected vmPFC cells [t test: $t(8) = 5.22$, $P < 0.01$ versus pre-light, $n = 8$ units] (Fig. 1D).

Next, to examine the effects of optogenetic manipulation of vmPFC inputs to the amygdala, we performed ex vivo slice electrophysiological recordings from BL pyramidal neurons. This revealed that blue light shone on the axons of ChR2-expressing vmPFC cells in the BL

(Fig. 1E) generated large excitatory postsynaptic currents (EPSCs) capable of triggering action potentials in BL neurons, in a light intensity–dependent manner ($F_{6,96} = 90.07$, $P < 0.01$, $n = 17$ recorded cells) (Fig. 1F). We also found that the light-evoked currents at the pyramidal neurons were blocked by application of the AMPA receptor antagonist CNQX, indicating that vmPFC-to-amygdala transmission was glutamatergic in nature ($F_{7,42} = 150.16$, $P < 0.01$, $n = 7$ recorded cells) (Fig. 1G). These data confirm and extend other studies showing that the BL is a major physiological target of the vmPFC (13, 19) and lend further credence to the notion that the BL is an initial locus of excitatory vmPFC inputs to the amygdala, which in turn drive activity at mICNs to inhibit CeA output (14, 19–21).

Consistent with prior anatomical tracing studies (16, 22, 23), close inspection of the pattern of vmPFC innervation in the amygdala revealed fluorescently labeled ChR2- and ArchT-expressing vmPFC axons in the BL, basomedial nucleus (BM), and the vicinity of mICN, which were visualized by immunostaining for the ICN marker FoxP2 (24, 25) (Fig. 1, H and I).

Given that our electrophysiological data indicated strong functional vmPFC inputs to the BL, we next chronically implanted ferrules bilaterally directing optical fibers and light at the BL and mICN (Fig. 1, J and K) to manipulate vmPFC inputs in vivo. Our goal was to selectively manipulate vmPFC inputs to this area of the amygdala, although we cannot exclude the possibility that fiber stimulation produced antidromic actions at vmPFC neurons, with corollary effects on vmPFC projections to other brain regions (26, 27).

In our first behavioral experiment, we conditioned mice expressing ChR2-AAV or a YFP-AAV control virus to associate a tone with footshock. The following day, tone-evoked fear (freezing) was extinguished via 50 unreinforced tone presentations. To test whether extinction was augmented by stimulating the vmPFC-amygdala neurons, blue light (473 nm, 10 mW, 20 Hz, 5-ms pulses) was shone during each extinction tone presentation, and the next day, extinction retrieval was probed via five (light-free) unreinforced tone presentations (Fig. 2A). Freezing did not differ between the ChR2 and YFP groups during either extinction training [analysis of variance (ANOVA) group effect: $P > 0.05$; trial-block effect: $F_{1,22} = 133.89$, $P < 0.01$; $n = 14$ to 22] or retrieval (t test: $P > 0.05$) (Fig. 2B).

Whereas these data suggest a failure of vmPFC-amygdala stimulation to strengthen extinction, an effect may have been occluded by the effectiveness of the 50-tone ("full") training procedure at producing a level of extinction that was difficult to enhance further. To address this caveat, we replicated the experiment but limited the training to 10 tone presentations (Fig. 2C). Under these "partial" extinction conditions, the ChR2-AAV group again did not differ from controls during training (ANOVA group effect: $P > 0.05$; trial-block effect: $F_{1,11} = 34.19$, $P < 0.01$; $n = 5$ to 8) but did show significantly less freezing on the (light-free) extinction retrieval test [t test: $t(11) = 4.12$, $P < 0.01$] (Fig. 2D). Thus, stimulating vmPFC-amygdala neurons during extinction training facilitated the long-term formation of an otherwise partially formed extinction memory. These data closely converge with the recent finding that ChR2-mediated excitation of vmPFC cell bodies during extinction training also promotes subsequent retrieval (28), as well as earlier studies showing facilitation by electrical vmPFC stimulation (11, 12, 29, 30). Our current findings

demonstrate that the amygdala is at least one of the principal targets mediating these extinction-facilitating effects of vmPFC activation.

We next asked whether activating vmPFC inputs to the amygdala also improved the expression of an already formed extinction memory, given prior work supporting such a role (4, 9). In this design, ChR2-expressing mice were given partial extinction training in the absence of light, and then were tested for retrieval with blue light shone on the amygdala (Fig. 2E). Freezing on retrieval did not differ between the ChR2 and YFP groups (*t* test: *P* > 0.05), showing that driving the vmPFC-amygdala circuit did not promote extinction retrieval (Fig. 2F). Some explanations for this negative effect are that our partial extinction training protocol did not produce an extant extinction memory to augment on retrieval or that the pathway was not adequately stimulated to reveal an effect owing to the somewhat limited ChR2-AAV expression in deep-layer vmPFC neurons that project to the amygdala (16, 22). Another possibility is that the predominant role of the vmPFC-amygdala pathway is to regulate the formation, but not the retrieval, of extinction memories. A selective, "instructional" role for this pathway could also account for the lack of effects of ChR2 stimulation on the expression of fear memories; an effect that has been observed with direct vmPFC stimulation in some earlier studies (28, 29).

Our ChR2 data demonstrate that stimulating the vmPFC-amygdala circuit is sufficient to bolster extinction memory formation but does not address the necessity of the circuit for extinction. Therefore, to test for circuit necessity, we shone green light (532 nm, 10 mW, continuous) on the amygdala to silence ArchT-expressing vmPFC axons during full, 50-tone extinction training (Fig. 3A). Freezing during extinction training did not differ between the ArchT and YFP groups (ANOVA group effect: *P* > 0.05; trial-block effect: $F_{1,16} = 24.43$, *P* < 0.01; *n* = 8 to 10). However, freezing in the ArchT group was significantly higher than controls during a light-free retrieval test [$t(16) = 2.96$, *P* < 0.01] (Fig. 3B), consistent with a deficit in long-term extinction.

Next, we silenced the vmPFC-amygdala pathway during retrieval, rather than extinction training (Fig. 3C). We found that freezing was unaltered by shining green light on the amygdala during retrieval (*t* test: *P* > 0.05) (Fig. 3D). These ArchT-silencing experiments mirror the effects of ChR2 activation by showing that vmPFC neurons projecting to the amygdala are necessary for long-term extinction memory formation, but not for extinction retrieval. Previous work has demonstrated that the vmPFC is active during cued extinction retrieval (29, 31, 32), and pharmacological inactivation of the vmPFC disrupts retrieval of a contextual extinction memory (33). As such, the lack of effect of vmPFC-amygdala silencing on retrieval suggests that vmPFC projections to other brain regions fulfill this role. Arguing against this, however, a recent study demonstrated that optogenetically silencing or pharmacologically inactivating cell bodies in the vmPFC itself also failed to disrupt extinction retrieval in rats, but did, as in the current study, impair extinction formation (28) [see also (34)]. Thus, whereas the vmPFC and its projections to the BL appear to be important for the retrieval of extinguished context-related fear, this circuit is dispensable for retrieving cued extinction memories.

We next sought to identify changes in amygdala activation associated with the ArchT-induced impairment in extinction, given earlier evidence that successful extinction is associated with robust LA and BL recruitment, and stimulating the VMPFC (electrically, pharmacologically) is sufficient to drive activation of these same amygdala nuclei. To this end, we repeated our experimental design in which we shone green light on ArchT-expressing vmPFC axons in the amygdala during full extinction training. We then probed retrieval (light-free) the following day and, 2 hours later, quantified the number of amygdala neurons positive for the immediate-early gene Zif268 (Fig. 3E). We found that the ArchT group froze significantly more ($42.3 \pm 5.9\%$) than YFP controls ($27.8 \pm 2.5\%$) during retrieval [$t(18) = 2.27$, $P < 0.05$, $n = 10$)], replicating our earlier experiment. In tandem with these behavioral deficits, we counted significantly fewer Zif268-positive neurons in the lateral amygdala (LA) [$t(13) = 2.44$, $P < 0.05$, $n = 7$ to 8] (Fig. 3F) and BL [$t(15) = 2.37$, $P < 0.05$, $n = 8$ to 9] (Fig. 3G) of the ArchT group compared with YFP controls. These data demonstrate that silencing vmPFC inputs to the amygdala attenuates recruitment of the LA and BL during extinction (11, 15).

In conclusion, the current study provides some of the first support for a causal role of the vmPFC-amygdala pathway in extinction memory formation, but not necessarily their retrieval. We report that optogenetically stimulating vmPFC inputs drives glutamatergic transmission in the BL and facilitates extinction acquisition, whereas silencing the vmPFC-amygdala pathway impairs extinction acquisition. Collectively, our data support an emerging model in which the vmPFC instructs changes in the BL and LA (35–37), leading to the formation of extinction memories and the dampening of fear via modulation of activity in the mICNs and CeA. Given the anatomical and functional similarities in the extinction-mediating circuits in rodents and humans (5, 38), our findings offer new insight into the pathophysiology of impaired extinction and persistent anxiety in disorders such as posttraumatic stress disorder.

METHODS

Subjects

Male adult C57BL/6J mice were singly housed (to maintain the integrity of intracranial implants) in a temperature- and humidity-controlled vivarium under a 12-hour light/dark cycle (lights on 0600). Experimental procedures were performed in accordance with the National Institutes of Health (NIH) *Guide for the Care and Use of Laboratory Animals* and approved by the local National Institute on Alcohol Abuse and Alcoholism (NIAAA) and Vanderbilt Animal Care and Use Committees. The number of mice used in each experiment is indicated in the main text.

Viral infusion and ferrule implantation

Mice were placed in a stereotaxic alignment system (Kopf Instruments) to infuse virus and implant ferrules. AAVs were bilaterally infused into the vmPFC using a Neuro syringe with a 33-gauge needle (Hamilton) at a rate of 0.02 μl/min and left in place for an additional 5 min [coordinates relative to bregma: AP (anteroposterior) +1.8, ML (mediolateral) +0.3, DV (dorsoventral) −2.8]. To express the excitatory ChR2 (39), we used rAAV5/CaMKII-

hChR2(H134R)-eYFP (0.18 μl per hemisphere; titer: 1×10^{13}). To express the inhibitory proton pump archaerhodopsin (40), we used rAAV5/CaMKII-eArchT3.0-eYFP (0.2 μl per hemisphere; titer: 8×10^{12}). As a control AAV, we used rAAV5/CaMKII-eYFP (0.22 μl per hemisphere; titer: 6×10^{12}). Viruses were purchased from the University of North Carolina vector core (www.med.unc.edu/genetherapy/vectorcore). Fiber optics of 200-mm diameter (numerical aperture, 0.37) were bilaterally directed at the amygdala (coordinates relative to bregma: AP +1.45, ML +3.25, DV –4.7) and chronically implanted by affixing to the skull with dental cement. Ferrule-fiber assembly was constructed according to previously published methods (41). Mice were left undisturbed for 5 to 6 weeks before testing to allow for recovery and virus expression.

To verify virus expression and ferrule placements at the completion of testing, mice were terminally overdosed with ketamine/xylazine and transcardially perfused with phosphate-buffered saline (PBS), then 4% paraformaldehyde (PFA). After suspension in 4% PFA overnight and in 0.1 M phosphate buffer at 4°C for 1 to 2 days, 50-μm coronal sections were cut with a vibratome (Classic 1000 model, Vibratome). Brain sections were incubated in 1% sodium borohydride followed by blocking solution [10% normal goat serum (Vector Laboratories) and 2% bovine serum albumin (MP Biomedicals) in 0.05 M PBS with 0.2% Triton X-100] for 2 hours at room temperature (20°C) and then incubated at 4°C overnight in a cocktail of primary antibodies: (i) chicken anti-GFP (1:3000 dilution, Abcam cat. no. 13970) to aid visualization of AAVs, and (ii) rabbit anti-FoxP2 (1:2000 dilution, Abcam cat. no. 16046) to visualize ICNs (24, 25). The next day, the sections were incubated in a cocktail of secondary antibodies: Alexa 488 goat anti-chicken immunoglobulin G (1:1000 dilution, Abcam cat. no. 150169) and TRITC goat anti-rabbit (1:1000 dilution, Abcam cat. no. 6719). The sections were mounted and coverslipped with Vectashield HardSet mounting medium with 4′,6-diamidino-2-phenylindole (Vector Laboratories Inc.). The sections were imaged with an Olympus BX41 microscope (Olympus) and a Zeiss LSM 700 confocal microscope (Carl Zeiss Microscopy).

In vivo multielectrode array recordings

To confirm virus efficacy in vivo, we conducted recordings of vmPFC single-unit activity during concurrent light on and off periods. Mice were infused with rAAV5/CaMKII-hChR2(H134R)-eYFP-AAV or rAAV5/CaMKII-hChR2(H134R)-eYFP-AAV, as described above, and implanted under isoflurane anesthesia with microelectrodes, using a stereotaxic alignment system (Kopf Instruments). The ferrule-fiber assembly was attached to a 16×2–row array (200-μm spacing between rows) of tungsten microelectrodes (Innovative Neurophysiology), such that the fiber tip was positioned about 0.5 mm above the wire tips (42). The array was inserted lengthwise anteroposterior (35-μm diameter, 150-μm spacing between electrodes within a row) in the left hemisphere. The coordinates for the center of the array were +1.8 mm anteroposterior, +0.35 μm mediolateral, and –2.9 dorsoventral from the bregma skull surface. The array coupled to optical fiber was fixed to the skull with screws and dental cement (Coralite Dental Products).

Five to 6 weeks after surgery, recordings were made as mice freely moved around a small cage, using the OmniPlex D Neural Data Acquisition System (Plexon). Laser power was

calibrated before each recording to ~10 mW. In ChR2-infected mice, blue-light ($\lambda = 473$ nm) pulses were delivered at 20 Hz in a cycled fashion: 1 s on/3 s off, repeated 100 to 200 times. In ArchT-infected mice, green light ($\lambda = 532$ nm) was delivered continuously for 30 s, interspersed by 5-s intervals, for a total of 25 to 30 iterations. The delivery of light was timestamped in the electrophysiological record, and waveforms were sorted off-line using two-dimensional plots of principal components, with waveform clusters marked in these plots with contours, using the Offline Sorter program (Plexon). Data were imported to the NeuroExplorer program (Nex Technologies), and Z-scores were normalized to baseline. Peri-event time histograms were generated in 50- and 500-ms bins for ChR2- and ArchT-injected mice, respectively.

To verify electrode placements at the completion of testing, mice were terminally anesthetized with ketamine/xylazine, and lesions were made at the tips of the recording electrodes by passing currents, typically 50 to 100 µA, for 20 s (S48 Stimulator and Model CCU1, Grass Technologies). Mice were transcardially perfused with 4% PFA solution in phosphate buffer, and brains were removed. Coronal sections (50 mm) were cut with a vibratome (Classic 1000 model, Vibratome) and stained with cresyl violet. Lesion sites were estimated with the aid of an Olympus (Center Valley) BX41 microscope.

Ex vivo slice electrophysiology recordings

Slice electrophysiological recordings were conducted at the Vanderbilt University Medical Center. Mice were placed in a stereotaxic alignment system (Stoelting) to infuse AAV9/ CaMKII-hChR2(H134R)-eYFP. WPRE.hGH-AAV (0.1 µl per hemisphere; titer: 1×1.98^{13}) (Penn Vector Core) (www.med.upenn.edu/gtp/vectorcore/), using the same coordinates as described above. At least 4 weeks later, mice were anesthetized with isoflurane and transcardially perfused with ice-cold cutting solution (containing 93 mM N-methyl-D-glucamine, 2.5 mM KCl, 20 mM Hepes, 3 mM Na-pyruvate, 10 mM $MgSO_4$ heptahydrate, 1.2 mM NaH_2PO_4, 30 mM $NaHCO_3$, 25 mM glucose, 5 mM Na-ascorbate, 0.5 mM $CaCl_2$ dihydrate, 3 mM N-acetylcysteine). Brains were removed, and coronal sections (250 µm) of the vmPFC and BL were collected using a Leica VT1000S vibratome (Leica Microsystems) in a 1° to 4°C oxygenated [95% (v/v) O_2, 5% (v/v) CO_2] bath of cutting solution. Slices were placed in a holding chamber containing the same cutting solution at 34°C for 10 min and then transferred to a chamber containing holding artificial cerebrospinal fluid (ACSF) (92 mM NaCl, 2.5 mM KCl, 20 mM Hepes, 3 mM Na-pyruvate, 2 mM $MgSO_4$ heptahydrate, 1.2 mM NaH_2PO_4, 30 mM $NaHCO_3$, 25 mM glucose, 5 mM Na-ascorbate, 2 mM $CaCl_2$ dihydrate, 3 mM N-acetylcysteine) at 24°C. Slices were allowed to recover for 20 min in holding ACSF before use.

For recording, slices were constantly perfused with oxygenated extracellular recording ACSF (113 mM NaCl, 2.5 mM KCl, 1.2 mM $MgSO_4$ heptahydrate, 2.5 mM $CaCl_2$ dihydrate, 1 mM NaH_2PO_4, 26 mM $NaHCO_3$, 3 mM Na-pyruvate, 1 mM Na-ascorbate, 20 mM glucose). Recording ACSF was perfused at a rate of 2 to 3 ml/min. For all experiments, the recording ACSF contained the g-aminobutyric acid type A ($GABA_A$) receptor antagonist picrotoxin (50 µM) to isolate glutamatergic transmission. For EPSC measurements, recording ACSF containing picrotoxin and the N-methyl-D-aspartate receptor antagonist

[D.L-2-amino-5-phosphonovaleric acid (APV), 50 μM] was used to decrease the late component of compound EPSC current density, as previously described (43).

Whole-cell voltage clamp and current clamp recordings were performed on BL pyramidal neurons and interneurons. Pyramidal neurons were identified by their triangular cell shape, large size, and large capacitance transient decay. Borosilicate glass patch electrodes were pulled using a Flaming/Brown microelectrode puller (Sutter Instrument) with a resistance between 3 and 5 megohms. For measurements of optically evoked action potentials, cells were current-clamped with a K-Glu–based intracellular solution [125 mM K-Glu, 4 mM NaCl, 10 mM Hepes, 4 mM Mg- ATP (adenosine triphosphate), 0.3 mM Na-GTP (guanosine triphosphate), 10 mM Na-phosphocreatine] and stimulated with 1 ms of blue wavelength (~473 nm) light using a M00257386 LED driver (Thorlabs). For measurements of optically evoked EPSCs, cells were voltage-clamped at −70 mV with a Cs-Glu–based intracellular solution (117 mM D-gluconate, 117 mM CsOH, 20 mM Hepes, 0.4 mM EGTA, 5 mM tetraethylammonium, 2 mM MgCl, 4 mM Na-ATP, 0.3 mM Na-GTP, 5 mM QX-314 bromide) and stimulated with 10-ms light pulses. Input/output EPSC amplitude was averaged for five stimulations (0.1 Hz) at six different LED intensities for each cell. To verify that transmission at the recorded pyramidal neurons was glutamatergic, light-evoked EPSCs were recorded with ACSF containing 50 μM of the AMPA receptor antagonist CNQX, perfused onto slices for 5 min after a 3-min drug-free baseline.

Behavioral testing

To habituate mice to being connected to the optic-fiber cables, they were handled for 2 min a day for 6 days before testing and were also connected to the cables in the home cage for 40 min a day for 3 days before testing. Fear conditioning was conducted in a 30 × 25 × 25–cm chamber with metal walls and a metal rod floor (context A), as previously described (44). To provide a distinctive olfactory cue, context A was cleaned between subjects with a 79.5% water:19.5% ethanol:1% vanilla extract solution. After a 120- to 180-s acclimation period, the mouse received three pairings (60- to 90-s inter-trial interval) between a 30-s, 80-dB white noise cue [conditioned stimulus (CS)] and a 0.6-mA scrambled footshock [unconditioned stimulus (US)] presented during the last 2 s of the tone. Mice remained in the chamber for 120 s after the final pairing. CS and US presentation was controlled by the Med Associates Freeze Monitor system (Med Associates Inc.).

Fear extinction acquisition was tested in a 27 × 27 × 14–cm chamber with transparent walls and a floor covered with wooden chips, cleaned between subjects with a 99% water:1% acetic acid solution, and housed in a different room from training (context B). After a 180-s acclimation period, there were either 10 ("partial extinction") or 50 ("full extinction") × 30-s CS presentations (5-s inter-CS interval). Freezing was defined as the absence of any visible movement, except that required for respiration, and was scored at 5-s intervals by an observer blind to genotype. The number of observations scored as freezing was converted to a percentage [(number of freezing observations/total number of observations) × 100] for analysis. The next day, extinction retrieval was tested in context B via 5 × 30–s CS presentations (5-s inter-CS interval) after 180 s of context acclimation.

To stimulate vmPFC-amygdala neurons, blue light ($\lambda = 473$ nm) was bilaterally shone at 20 Hz on ChR2-infected axons in the amygdala throughout the duration of 30-s CS presentations. Light was shone in this manner either during each of 10× (partial extinction experiment, schematized in Fig. 1C) or 50× CS (full extinction experiment, schematized in Fig. 1A) extinction training trials or during 5× CS extinction retrieval trials (extinction retrieval experiment, schematized in Fig. 1E).

To silence vmPFC-amygdala neurons, green light ($\lambda = 532$ nm) was bilaterally shone continuously on ArchT-infected axons in the amygdala throughout the duration of 30-s CS presentations. Light was shone in this manner either during each of 50× CS (extinction training experiment, schematized in Fig. 2C) extinction training trials or during 5× CS extinction retrieval trials (extinction retrieval experiment, schematized in Fig. 2E).

The power of the blue and green laser was ~10 mW measured at the tip of the optic fiber. Laser power was calibrated before each experiment by measuring the power at the tip of the patch cord with a PM100D optical power meter with an S120C sensor (Thorlabs) and multiplying that power by the transmittance of the ferrule connection on each optrode.

Immediate-early gene mapping

Activation of cells positive for the plasticity-related immediate-early gene Zif268 was examined in amygdala subregions after behavioral testing, as previously described (45, 46). ArchT- and YFP-infected mice were fear-conditioned and given full (50-trial) extinction training with green light shone during each CS presentation, followed by a light-free retrieval test the next day, as described above (schematized in Fig. 3E). Two hours after extinction retrieval, mice were sacrificed via cervical dislocation and rapid decapitation, and brains were flash-frozen. Brains were sectioned in the coronal plane at 20-μm thickness on a cryostat (CM1850, Leica Microsystems) and collected on gelatin-coated slides.

Sections were postfixed in 4% PFA (for 30 min) and preincubated in normal goat serum (for 30 min). Sections were then incubated overnight with a rabbit anti-Zif268 polyclonal primary antibody (1:2500; sc-189, Santa Cruz Biotechnology) and a biotinylated goat anti-rabbit secondary antibody (1:200; Vector Laboratories). An avidin–biotin–horseradish peroxidase procedure (Vectastain ABC Kit, Vector Laboratories) with 3,3′-diaminobenzidine (Sigma) as chromogen was used to visualize Zif268-positive cells. The anatomical localization of Zif268-positive cells was made with reference to a mouse stereotaxic atlas. Cells containing a nuclear brown-black reaction product were considered to be Zif268-positive cells and counted, bilaterally, within the whole subregion using a light microscope (Olympus BX-40), then calculated as means in a representative 0.01-mm^2 area of tissue.

Statistical analyses

The effects of virus group × CS bin on freezing during fear conditioning and extinction training were analyzed via two-factor ANOVA. The effect of virus group on levels of freezing during retrieval and the number of Zif268-labeled cells were analyzed using

Student's *t* tests. The effect of light on *z*-scored unit activity was analyzed using paired *t* tests. The threshold for statistical significance was set at $P < 0.05$.

Acknowledgments

REFERENCES AND NOTES

1. American Psychiatric Association. DSM-5, Diagnostic and Statistical Manual of Mental Disorders. Vol. 4. APA Press; Washington, DC: 2013.

2. Holmes A, Singewald N. Individual differences in recovery from traumatic fear. Trends Neurosci. 2013; 36:23–31. [PubMed: 23260015]

3. Rozeske RR, Valerio S, Chaudun F, Herry C. Prefrontal neuronal circuits of contextual fear conditioning. Genes Brain Behav. 2015; 14:22–36. [PubMed: 25287656]

4. Duvarci S, Pare D. Amygdala microcircuits controlling learned fear. Neuron. 2014; 82:966–980. [PubMed: 24908482]

5. Milad MR, Quirk GJ. Fear extinction as a model for translational neuroscience: Ten years of progress. Annu. Rev. Psychol. 2012; 63:129–151. [PubMed: 22129456]

6. Lüthi A, Lüscher C. Pathological circuit function underlying addiction and anxiety disorders. Nat. Neurosci. 2014; 17:1635–1643. [PubMed: 25402855]

7. Stafford JM, Maughan DK, Ilioi EC, Lattal KM. Exposure to a fearful context during periods of memory plasticity impairs extinction via hyperactivation of frontal-amygdalar circuits. Learn. Mem. 2013; 20:156–163. [PubMed: 23422280]

8. Herry C, Johansen JP. Encoding of fear learning and memory in distributed neuronal circuits. Nat. Neurosci. 2014; 17:1644–1654. [PubMed: 25413091]

9. Orsini CA, Maren S. Neural and cellular mechanisms of fear and extinction memory formation. Neurosci. Biobehav. Rev. 2012; 36:1773–1802. [PubMed: 22230704]

10. Fitzgerald PJ, Whittle N, Flynn SM, Graybeal C, Pinard CR, Gunduz-Cinar O, Kravitz AV, Singewald N, Holmes A. Prefrontal single-unit firing associated with deficient extinction in mice. Neurobiol. Learn. Mem. 2014; 113:69–81. [PubMed: 24231425]

11. Maroun M, Kavushansky A, Holmes A, Wellman C, Motanis H. Enhanced extinction of aversive memories by high-frequency stimulation of the rat infralimbic cortex. PLOS One. 2012; 7:e35853. [PubMed: 22586453]

12. Vidal-Gonzalez I, Vidal-Gonzalez B, Rauch SL, Quirk GJ. Microstimulation reveals opposing influences of prelimbic and infralimbic cortex on the expression of conditioned fear. Learn. Mem. 2006; 13:728–733. [PubMed: 17142302]

13. Cho JH, Deisseroth K, Bolshakov VY. Synaptic encoding of fear extinction in mPFC-amygdala circuits. Neuron. 2013; 80:1491–1507. [PubMed: 24290204]

14. Amano T, Unal CT, Paré D. Synaptic correlates of fear extinction in the amygdala. Nat. Neurosci. 2010; 13:489–494. [PubMed: 20208529]

15. Amir A, Amano T, Pare D. Physiological identification and infralimbic responsiveness of rat intercalated amygdala neurons. J. Neurophysiol. 2011; 105:3054–3066. [PubMed: 21471396]

16. Gabbott PL, Warner TA, Jays PR, Salway P, Busby SJ. Prefrontal cortex in the rat: Projections to subcortical autonomic, motor, and limbic centers. J. Comp. Neurol. 2005; 492:145–177. [PubMed: 16196030]

17. McDonald AJ, Mascagni F, Guo L. Projections of the medial and lateral prefrontal cortices to the amygdala: A Phaseolus vulgaris leucoagglutinin study in the rat. Neuroscience. 1996; 71:55–75. [PubMed: 8834392]

18. Sotres-Bayon F, Quirk GJ. Prefrontal control of fear: More than just extinction. Curr. Opin. Neurobiol. 2010; 20:231–235. [PubMed: 20303254]

19. Strobel C, Marek R, Gooch HM, Sullivan RK, Sah P. Prefrontal and auditory input to intercalated neurons of the amygdala. Cell Rep. 2015; 10:1435–1442.

20. Smith Y, Paré JF, Paré D. Differential innervation of parvalbumin-immunoreactive inter-neurons of the basolateral amygdaloid complex by cortical and intrinsic inputs. J. Comp. Neurol. 2000; 416:496–508. [PubMed: 10660880]

21. Brinley-Reed M, Mascagni F, McDonald AJ. Synaptology of prefrontal cortical projections to the basolateral amygdala: An electron microscopic study in the rat. Neurosci. Lett. 1995; 202:45–48. [PubMed: 8787827]

22. Vertes RP. Differential projections of the infralimbic and prelimbic cortex in the rat. Synapse. 2004; 51:32–58. [PubMed: 14579424]

23. Pinard CR, Mascagni F, McDonald AJ. Medial prefrontal cortical innervation of the intercalated nuclear region of the amygdala. Neuroscience. 2012; 205:112–124. [PubMed: 22249157]

24. Busti D, Geracitano R, Whittle N, Dalezios Y, Ma ko M, Kaufmann W, Sätzler K, Singewald N, Capogna M, Ferraguti F. Different fear states engage distinct networks within the intercalated cell clusters of the amygdala. J. Neurosci. 2011; 31:5131–5144. [PubMed: 21451049]

25. Kaoru T, Liu FC, Ishida M, Oishi T, Hayashi M, Kitagawa M, Shimoda K, Takahashi H. Molecular characterization of the intercalated cell masses of the amygdala: Implications for the relationship with the striatum. Neuroscience. 2010; 166:220–230. [PubMed: 20004711]

26. Tye KM, Prakash R, Kim SY, Fenno LE, Grosenick L, Zarabi H, Thompson KR, Gradinaru V, Ramakrishnan C, Deisseroth K. Amygdala circuitry mediating reversible and bidirectional control of anxiety. Nature. 2011; 471:358–362. [PubMed: 21389985]

27. Jennings JH, Sparta DR, Stamatakis AM, Ung RL, Pleil KE, Kash TL, Stuber GD. Distinct extended amygdala circuits for divergent motivational states. Nature. 2013; 496:224–228. [PubMed: 23515155]

28. Do-Monte FH, Manzano-Nieves G, Quiñones-Laracuente K, Ramos-Medina L, Quirk GJ. Revisiting the role of infralimbic cortex in fear extinction with optogenetics. J. Neurosci. 2015; 35:3607–3615. [PubMed: 25716859]

29. Milad MR, Quirk GJ. Neurons in medial prefrontal cortex signal memory for fear extinction. Nature. 2002; 420:70–74. [PubMed: 12422216]

30. Kim SC, Jo YS, Kim IH, Kim H, Choi JS. Lack of medial prefrontal cortex activation underlies the immediate extinction deficit. J. Neurosci. 2010; 30:832–837. [PubMed: 20089891]

31. Holmes A, Fitzgerald PJ, MacPherson KP, DeBrouse L, Colacicco G, Flynn SM, Masneuf S, Pleil KE, Li C, Marcinkiewcz CA, Kash TL, Gunduz-Cinar O, Camp M. Chronic alcohol remodels prefrontal neurons and disrupts NMDAR-mediated fear extinction encoding. Nat. Neurosci. 2012; 15:1359–1361. [PubMed: 22941108]

32. Knapska E, Macias M, Mikosz M, Nowak A, Owczarek D, Wawrzyniak M, Pieprzyk M, Cymerman IA, Werka T, Sheng M, Maren S, Jaworski J, Kaczmarek L. Functional anatomy of neural circuits regulating fear and extinction. Proc. Natl. Acad. Sci. U.S.A. 2012; 109:17093–17098. [PubMed: 23027931]

33. Laurent V, Westbrook RF. Inactivation of the infralimbic but not the prelimbic cortex impairs consolidation and retrieval of fear extinction. Learn. Mem. 2009; 16:520–529. [PubMed: 19706835]

34. Sierra-Mercado D, Padilla-Coreano N, Quirk GJ. Dissociable roles of prelimbic and infralimbic cortices, ventral hippocampus, and basolateral amygdala in the expression and extinction of conditioned fear. Neuropsychopharmacology. 2011; 36:529–538. [PubMed: 20962768]

35. Jüngling K, Seidenbecher T, Sosulina L, Lesting J, Sangha S, Clark SD, Okamura N, Duangdao DM, Xu YL, Reinscheid RK, Pape HC. Neuropeptide S-mediated control of fear expression and extinction: Role of intercalated GABAergic neurons in the amygdala. Neuron. 2008; 59:298–310. [PubMed: 18667157]

36. Repa JC, Muller J, Apergis J, Desrochers TM, Zhou Y, LeDoux JE. Two different lateral amygdala cell populations contribute to the initiation and storage of memory. Nat. Neurosci. 2001; 4:724–731. [PubMed: 11426229]

37. Herry C, Ciocchi S, Senn V, Demmou L, Müller C, Lüthi A. Switching on and off fear by distinct neuronal circuits. Nature. 2008; 454:600–606. [PubMed: 18615015]

38. Singewald N, Schmuckermair C, Whittle N, Holmes A, Ressler KJ. Pharmacology of cognitive enhancers for exposure-based therapy of fear, anxiety and trauma-related disorders. Pharmacol. Ther. 2015; 149:150–190. [PubMed: 25550231]

39. Zhang F, Wang LP, Brauner M, Liewald JF, Kay K, Watzke N, Wood PG, Bamberg E, Nagel G, Gottschalk A, Deisseroth K. Multimodal fast optical interrogation of neural circuitry. Nature. 2007; 446:633–639. [PubMed: 17410168]

40. Han X, Chow BY, Zhou H, Klapoetke NC, Chuong A, Rajimehr R, Yang A, Baratta MV, Winkle J, Desimone R, Boyden ES. A high-light sensitivity optical neural silencer: Development and application to optogenetic control of non-human primate cortex. Front. Syst. Neurosci. 2011; 5:18. [PubMed: 21811444]

41. Sparta DR, Stamatakis AM, Phillips JL, Hovelsø N, van Zessen R, Stuber GD. Construction of implantable optical fibers for long-term optogenetic manipulation of neural circuits. Nat. Protoc. 2012; 7:12–23. [PubMed: 22157972]

42. Kravitz AV, Owen SF, Kreitzer AC. Optogenetic identification of striatal projection neuron subtypes during in vivo recordings. Brain Res. 2013; 1511:21–32. [PubMed: 23178332]

43. Ammari R, Lopez C, Bioulac B, Garcia L, Hammond C. Subthalamic nucleus evokes similar long lasting glutamatergic excitations in pallidal, entopeduncular and nigral neurons in the basal ganglia slice. Neuroscience. 2010; 166:808–818. [PubMed: 20074618]

44. Fitzgerald PF, Pinard CR, Camp MC, Feyder M, Sah A, Bergstrom HC, Graybeal C, Liu Y, Schlüter OM, Grant SG, Singewald N, Xu W, Holmes A. Durable fear memories require PSD-95. Mol. Psychiatry. 2015; 20:901–912. [PubMed: 25510511]

45. Whittle N, Hauschild M, Lubec G, Holmes A, Singewald N. Rescue of impaired fear extinction and normalization of cortico-amygdala circuit dysfunction in a genetic mouse model by dietary zinc restriction. J. Neurosci. 2010; 30:13586–13596. [PubMed: 20943900]

46. Hefner K, Whittle N, Juhasz J, Norcross M, Karlsson RM, Saksida LM, Bussey TJ, Singewald N, Holmes A. Impaired fear extinction learning and cortico-amygdala circuit abnormalities in a common genetic mouse strain. J. Neurosci. 2008; 28:8074–8075. [PubMed: 18685032]
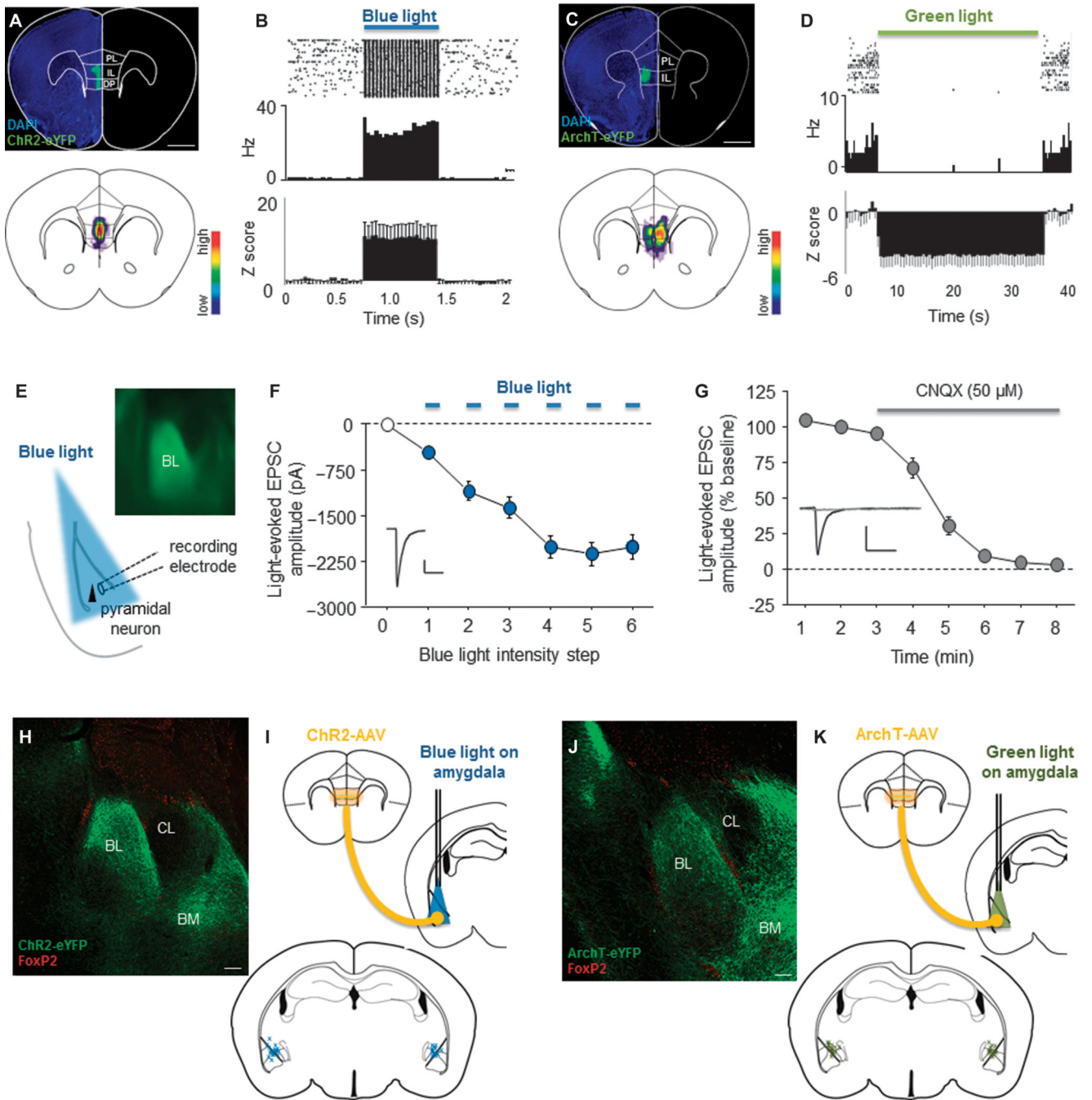
**Fig. 1. Bidirectional control of the vmPFC-amygdala circuit**

(**A** and **C**) Examples (top) and virus localization population heat maps representing all mice used in the current study (bottom; red and blue respectively represent maximum and minimum areas of cumulative virus localization across mice) of ChR2-AAV–expressing (A) and ArchT-AAV–expressing (C) glutamatergic neurons in vmPFC. Scale bar, 500 μm. (**B** and **D**) Raster plots and firing rate from single units (top), and z-scored population activity (bottom) showing blue-light (473 nm, 10 mW, 20 Hz, 5-ms pulses) increased (B) and green-light (532 nm, 10 mW, continuous) decreased (D) in vivo vmPFC unit activity in ChR2-

AAV– and ArchT-AAV–expressing neurons. (**E**) Example of slice containing ChR2-AAV–expressing vmPFC axons in the BL and cartoon depicting the procedure for recording blue light–evoked activity at BL pyramidal neurons. (**F**) Blue light shone on ChR2-AAV–expressing vmPFC axons in the BL increased EPSC amplitude at BL pyramidal neurons in a light intensity–dependent manner (scale bar: y axis, 500 pA; x axis, 50 ms). (**G**) Application of the AMPA receptor blocker CNQX abolished light-evoked EPSCs at BL pyramidal neurons (scale bar: y axis, 300 pA; x axis, 50 ms). (**H** and **J**) Examples of infected axons immunolabeled with anti–green fluorescent protein (GFP)/Alexa 488 antibodies (green) in the BL and BM of ChR2-AAV–expressing (H) and ArchT-AAV–expressing (J) vmPFC projection neurons. ICNs are immunolabeled with anti–Forkhead box protein P2 (FoxP2)–tetramethyl rhodamine isothiocyanate (TRITC) antibodies (red) (scale bars, 100 μm). (**I** and **K**) Cartoon depicting optic-fiber placement (top) and localization (bottom) targeting ChR2-AAV–expressing (I) and ArchT-AAV–expressing (K) vmPFC axons, representing all mice used in the current study. Data are means ± SEM.
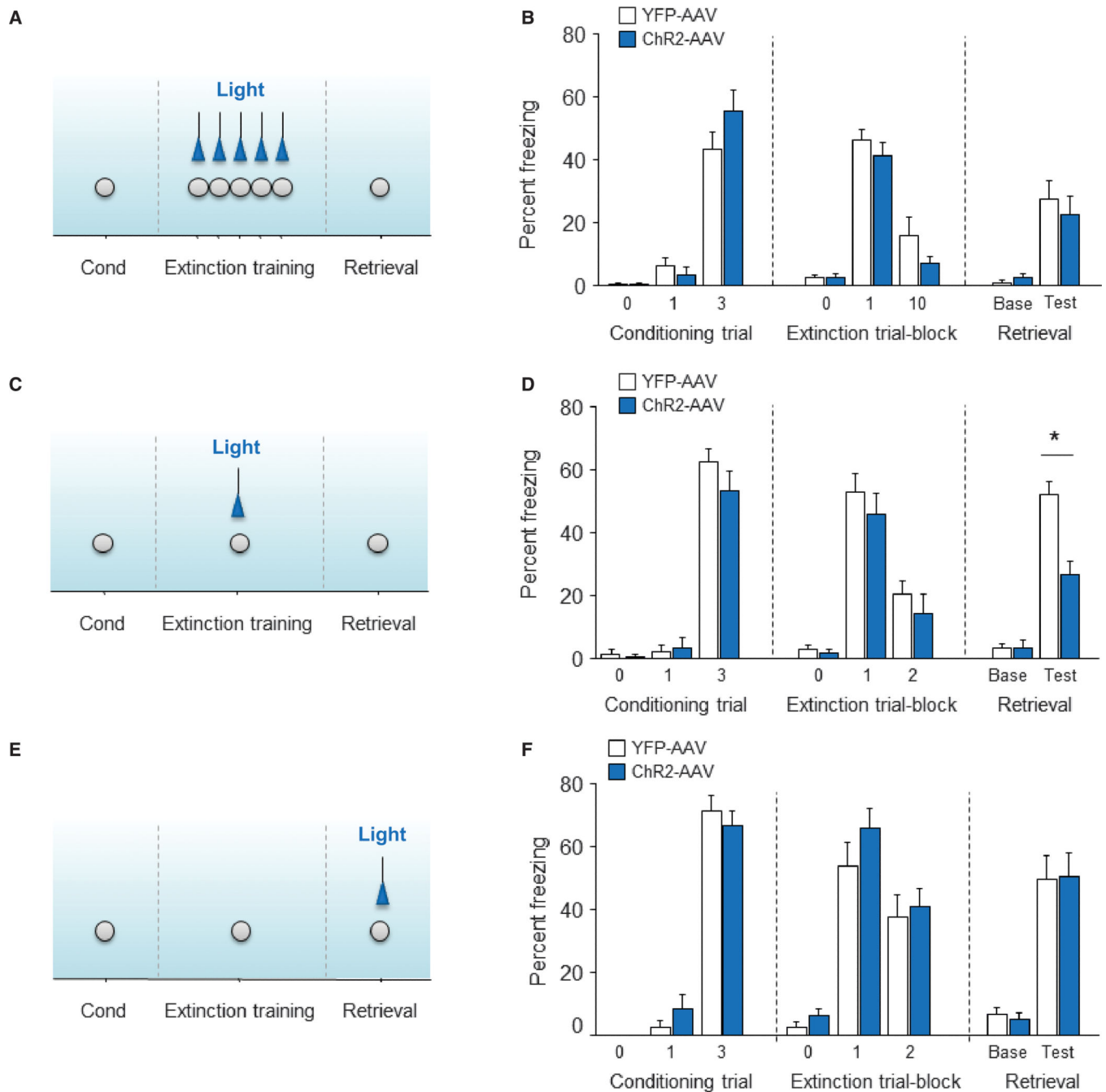
Fig. 2. vmPFC-amygdala circuit stimulation facilitates extinction formation

(**A** and **B**) Blue light shone on ChR2-AAV–expressing vmPFC axons in the amygdala during full (50-trial) extinction training (A) did not change freezing during training or subsequent (light-free) retrieval (B). (**C** and **D**) Light shone during partial (10-trial) extinction training (C) decreased freezing during (light-free) retrieval (D). (**E** and **F**) Light shone during retrieval [after partial (10-trial, light-free) extinction training] (E) did not alter freezing (F). For virus expression and optical fiber locations, see Fig. 1, A, H, and I. Extinction trial-block = 5 CS (conditioned stimulus) presentations.
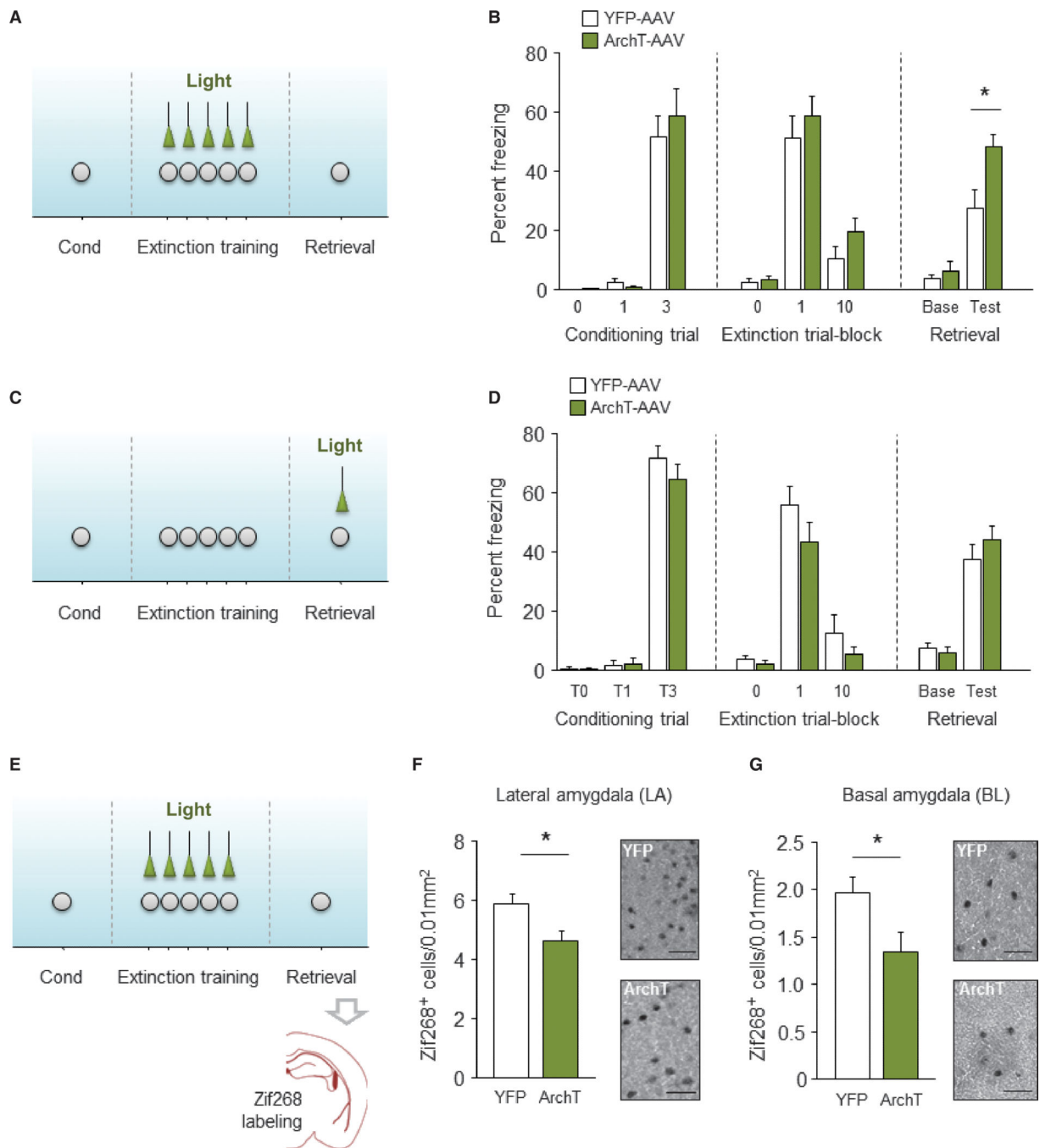
Fig. 3. vmPFC-amygdala circuit silencing impairs extinction formation and BL recruitment
(**A** and **B**) Green light shone on ArchT-AAV–expressing vmPFC axons in the amygdala
during extinction training (A) increased freezing during training or subsequent (light-free)
retrieval (B). (**C** and **D**) Light shone during retrieval (after light-free extinction training) (C)
did not alter freezing (D). (**E** to **G**) Green light shone during extinction training (E)
decreased the number of Zif268+ cells in the LA (F) and BL (G) (example images shown on

the right; scale bar, 50 μm). For virus expression and optical fiber locations, see Fig. 1, C, J, and K. Extinction trial-block = 5 CS presentations.